Hindawi
International Journal of Electrochemistry
Volume 2017, Article ID 5391794, 6 pages
https://doi.org/10.1155/2017/5391794

Research Article

Thermodynamics of Lithium Intercalation in Randomly Oriented High Graphene Carbon

Rahul S. Kadam and Kishor P. Gadkaree

Corning Incorporated, 1 Science Drive, Painted Post, NY 14870, USA

Correspondence should be addressed to Rahul S. Kadam; kadamrs@corning.com

Received 17 February 2017; Revised 27 April 2017; Accepted 18 May 2017; Published 15 June 2017

Academic Editor: Sheng S. Zhang

This paper covers details of systematic investigation of the thermodynamics (entropy and enthalpy) of intercalation associated with lithium ion in a structurally novel carbon, called Randomly Oriented High Graphene (ROHG) carbon and graphite. Equilibrated OCV (Open Circuit Voltage) versus temperature relationship is investigated to determine the thermodynamic changes with the lithium intercalation. ROHG carbon shows entropy of 9.36 $J \cdot mol^{-1} \cdot K^{-1}$ and shows no dependency on the inserted lithium concentration. Graphite shows initial entropy of 84.27 $J \cdot mol^{-1} \cdot K^{-1}$ and shows a strong dependence on lithium concentration. ROHG carbon (from −90.85 kJ mol^{-1} to −2.88 kJ mol^{-1}) shows gradual change in the slope of enthalpy versus lithium ion concentration plot compared to graphite (−48.98 kJ mol^{-1} to 1.84 kJ mol^{-1}). The study clearly shows that a lower amount of energy is required for the lithium ion intercalation into the ROHG structure compared to graphite structure. Randomly oriented graphene platelet cluster structure of ROHG carbon makes it easier for the intercalation or deintercalation of lithium ion. The ease of intercalation and the small cluster structure of ROHG as opposed to the long linear platelet structure of graphite lead to higher rates of the charge-discharge process for ROHG, when used as an electrode material in electrochemical applications.

1. Introduction

Lithium ion devices are currently being used in various applications such as automotive, hand-held, portable devices, aerospace, and solar applications. The lithium ion device basically involves three key components: anode (negative electrode), cathode (positive electrode), and electrolyte. All three of the components contribute equally to make the device perform at an optimum level. Failure of one of the components can cause the entire device to fail. Therefore, tremendous efforts to advance all the three components of a lithium ion device have been made. Novel materials have been invented and successfully used as anodes, cathodes, and electrolytes in lithium ion devices. Generally, the anode (negative electrode) consists of a lithium intercalating material such as graphite, hard carbon, soft carbon, or silicon which allows the lithium ions to be inserted in its matrix or structure. The energy storage mechanism depends on the efficiency of lithium storage and transport in the structure of the material [1–4].

Graphite has been the material of choice for the anode electrode in all commercial devices. A typical four-stage lithium intercalation curve in graphite material is well known in the literature (Figure 1).

Lithium intercalates in the structure of graphite to form Li-C compounds with varying stoichiometry, depending on voltage, which are known as graphite intercalation compounds (GIC). It is reported that lithium insertion occurs in steps and distinct phases are associated with each step. The different phases occur sequentially as stage 4, stage 3, stage 2, and stage 1. The mechanism and energy related to intercalation of lithium are entirely dependent on the structure of the substrate that the lithium intercalates in [5–11].

Each stage described above has free energy associated with it. Temperature dependence of Open Circuit Voltage (OCV) (electromotive force (emf)) is reported for Li-Sn system in the literature to measure free energy components (entropy and enthalpy) associated with the alloy [12]. With an assumption that lithium intercalated in graphite (or any

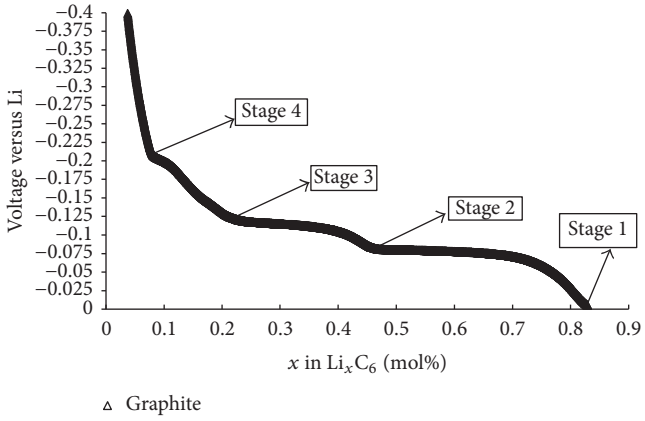

Figure 1: Four different stages in lithium intercalation in graphite.

carbon) forms a graphite intercalation compound, the same concept is applied to Li-C systems and is reported in the literature by Reynier et al. [13]. Using the fundamental laws of thermodynamics (1), the entropy (ΔS) and enthalpy (ΔH) associated with free energy of the lithium ion intercalation in the graphite structure is calculated from (2) and (3). Gibbs free energy (ΔG) is related to OCV and is temperature dependent as shown in (1) [12–14].

$$\Delta G(x) = -FE_0(x) = \Delta H(x) - T\Delta S(x), \quad (1)$$

where F is Faradays constant; T is absolute temperature; E_0 is OCV (Open Circuit Voltage)

Based on (1), the entropy is calculated by

$$\Delta S(x) = F\left(\frac{\delta E_0}{\delta T}\right)_x \quad (2)$$

and the enthalpy is calculated as

$$\Delta H(x) = -FE_0(x) + TF\left(\frac{\delta E_0}{\delta T}\right)_x, \quad (3)$$

where $(\delta E_0/\delta T)$ is slope for a temperature versus OCV plot.

In this work we report measurement of dependence of Open Circuit Voltage (OCV) on temperature and the entropy and enthalpy change associated with the free energy of lithium intercalation in the structure of an experimental carbon. Comparative data on graphite is also given. The nature of the curve for lithium intercalation in the structure of the carbon and the entropy and the enthalpy curves are explained based on structure for the novel carbon and lithium intercalation model for the carbon is also predicted. The experimental carbon is referred to as "Randomly Oriented High Graphene" (ROHG) carbon due to the unique structure of this carbon as determined from simulation of diffraction data carried out earlier.

2. Experimental

2.1. Materials. ROHG carbon was obtained from a natural carbon precursor via heat treatment in inert environment at temperatures above 1000°C.

Graphite powder specially synthesized for Li-ion electrode applications, Timcal (Model TB-17), was acquired from MTI Corporation and used as acquired.

KYNAR 761 grade PVDF was acquired from Arkema Chemicals Company. Timcal Super-C45 carbon black and lithium disc were acquired from MTI Corporation. N-Methyl pyrrolidinone was acquired from Sigma Aldrich.

2.2. Electrodes. The electrodes consisted of 90% carbon (ROHG or graphite Timcal (Model TB-17)), 5% Timcal Super-C45, and 5% PVDF (KYNAR -761). 3.6 grams of carbon and 0.2 grams of Timcal Super-C45 were ball milled for 10 minutes at 350 rpm in Retsch PM100. 0.2 grams of PVDF was added to the ball milled mixture and ball milled for another 10 minutes at 350 rpm. 5 ml of NMP (N-methyl pyrrolidinone) was added to the carbon, conductive carbon, and PVDF mixture and ball milled for 10 minutes at 350 rpm to yield a viscous slurry mixture. The slurry mixture was coated on a copper foil (product number Oak-Mitsui TLB-DS) acquired from Oak-Mitsui using the Mayer rod coating method (rod number 50 G). The coated electrodes were dried under vacuum at 50°C. The dried electrodes were punched into discs of 14 mm. The punched electrodes were dried under vacuum at 120°C for 12 hours. The electrodes were stored under Argon atmosphere in a glove box.

2.3. Half Cell Fabrication and Conditioning. Half cells (coin cells) were built with carbon (ROHG or graphite) electrodes and lithium metal disc as the counter electrodes. Polyethylene based separator was used to separate the two electrodes. 120 μl of 1.2 M LiPF6 in 20 : 20 : 60 ethylene carbonate : dimethyl carbonate : methyl propionate (volumetric) and 5 wt% fluoroethylene carbonate was used as an electrolyte. The cells were conditioned with two slow (~ C/30 rate) charge-discharge cycles on Arbin. During the first charge step, there was consumption of lithium to form the solid electrolyte interface (SEI). This phenomenon was seen around −1 V in the lithiation curve (Figure 4). The loss of lithium in the first charging step is also known as irreversible capacity. Since the first charge-discharge cycle was essentially used for conditioning the electrode to open up the interstices of the carbon in the electrode under test, the second cycle was the appropriate cycle to be considered for calculations.

2.4. Equilibration Time Determination. Experiments were performed to find the correct equilibration time. A minimum equilibration time is necessary to achieve a steady equilibrium among all the components of the cell at the given temperature and voltage and thus to obtain accurate data on the thermodynamic parameters. According to literature [13], 10 minutes' equilibrium time was sufficient and the OCV varied linearly with change in temperature at that equilibration time. We found that this does not hold true in our investigation and had to conduct a set of experiments to investigate the equilibration time. It is well known that linear change occurs in OCV with temperature as long as there is no phase change occurring in the system during intercalation [12]. Figure 2 shows the experimental data for ROHG at 2-hour and 4-hour equilibration time. The cell equilibrated at

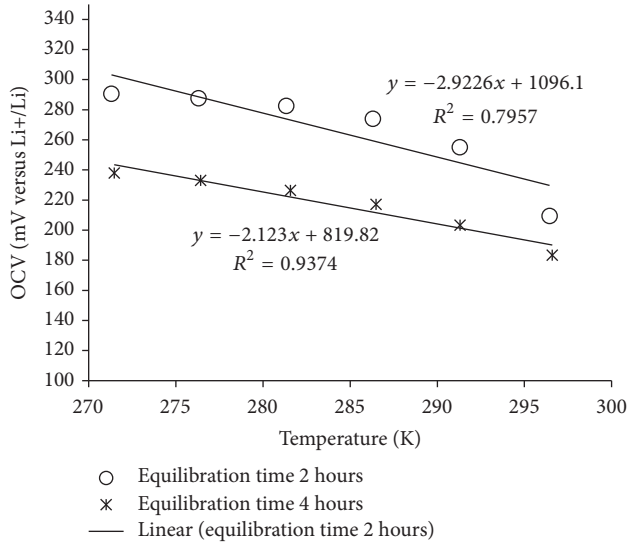

Figure 2: Plot of temperature (K) versus OCV for equilibration times.

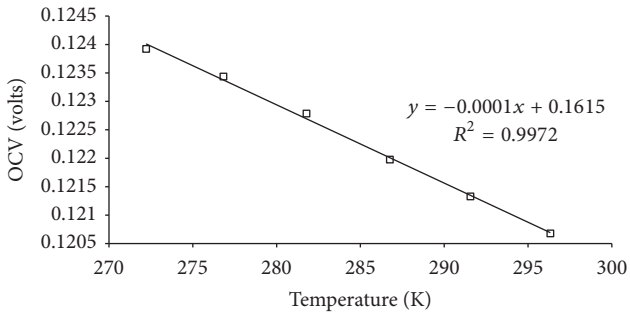

Figure 3: Plot of temperature (K) versus OCV (volts).

4-hour time showed R^2 value of 0.93 versus 0.79 for cells with 2-hour equilibration time. It is thus clear that at least 4-hour equilibration time is necessary to obtain good data. Four hours was thus chosen as the equilibration time for further studies.

2.5. OCV versus Temperature Behavior. The OCV versus temperature behavior for both ROHG and graphite was determined as follows. The OCV was measured for different temperatures at a given voltage. The measurements were done at a given cell voltage and at temperatures 0°C, 5°C, 10°C, 15°C, 20°C, and 25°C. An example of a typical variation in the OCV with temperature at a given voltage is shown in Figure 3. Similar plots were obtained for different cell voltages for the ROHG and graphite.

2.6. Calculation Method. The OCV versus temperature plot yielded a linear relationship and from the slope of the line ($\delta E_0/\delta T$) was calculated. The change in the voltage with temperature was used to calculate the entropy and enthalpy using (2) and (3), respectively.

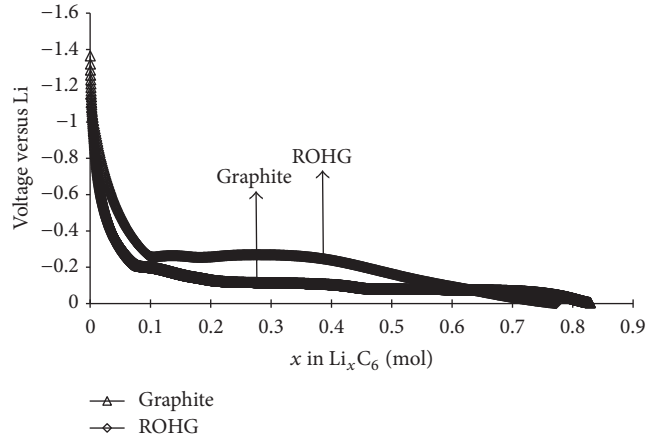

Figure 4: Plot of moles of Li versus voltage with reference to Li metal.

Table 1: Entropy and enthalpy data for ROHG at 296°K.

Voltage	Entropy (ΔS) J·mol^{-1}·K^{-1}	Enthalpy (ΔH) kJ·mol^{-1}	x in Li$_x$C$_6$
−0.013	−5.61	−2.88	0.741
−0.119	−0.56	−11.30	0.559
−0.250	9.36	−20.62	0.378
−0.500	9.36	−44.03	0.047
−0.750	9.36	−67.44	0.020
−1.000	9.36	−90.85	0.005

3. Results and Discussion

3.1. Intercalation Curves. Clearly, there is a difference in the lithium intercalation mechanism between ROHG and graphite as seen from Figure 4. Unlike graphite [8–10], only two stages are seen with the ROHG. Initially the voltage drops from starting OCV (−2.9 V) to −0.256 V and held at about that voltage as the plateau shows. At this stage, the Li-C stoichiometry is $Li_{0.188}C_6$. The second stage shows a continuous drop from −0.254 V to 0 V with a stoichiometry $Li_{0.78}C_6$. The different features associated with progression in lithium intercalation in the concentration versus voltage plot indicate that different lithium compounds are present in ROHG compared to graphite.

The equilibrium OCV is the potential difference between the two electrodes, that is, graphite or ROHG versus the lithium metal foil. Tables 1 and 2 show the relationship of OCVs and mole fraction of lithium in ROHG and graphite at 296°K, respectively. The OCV depends on the chemical environment where the lithium resides in the carbon structure on an atomic level. The half cells with ROHG carbon and graphite show similar trends in OCV with increase in lithium concentration/mole fraction (Figure 5). However, the change in the OCV is more gradual in the case of the ROHG carbon compared to the graphite after the initial OCV change at low concentration. This suggests that, unlike graphite, there is continuous change in the chemical environment in the ROHG carbon almost to the end compared to graphite, which

Table 2: Entropy and enthalpy data for graphite at 296°K.

Voltage	Entropy (ΔS) $J{\cdot}mol^{-1}{\cdot}K^{-1}$	Enthalpy (ΔH) $kJ{\cdot}mol^{-1}$	x in Li_xC_6
−0.004	7.49	1.84	0.829
−0.122	−9.36	−14.20	0.222
−0.217	4.68	−18.93	0.076
−0.482	74.91	−22.91	0.028
−0.800	84.27	−48.98	0.010

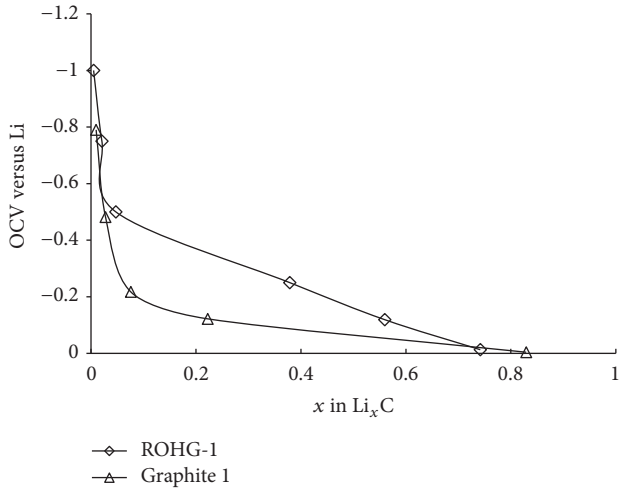

Figure 5: Relationship of Open Circuit Voltage (OCV) and mole fraction of lithium in carbon structure.

shows smaller change in the OCV with lithium intercalation after the initial change associated with lithium incorporation. This difference indicates that the mechanisms of lithium incorporation in ROHG and graphite are different.

3.2. Relationship between Entropy and Enthalpy with Lithium Intercalation. At a given voltage, the potential of the cell varies with the change in temperature. This fact can be used to measure the enthalpy and entropy contribution to the free energy of lithium intercalation and can be directly related to the lithium concentration in the carbon as reported in the literature [12, 13]. Figure 6 and Tables 1 and 2 shows the entropy and enthalpy contributions to the free energy of lithium intercalation in the ROHG and graphite, respectively. An assumption is made that lithium on the cathode (lithium metal electrode) is in excess and entropy and enthalpy changes occur only due to the change in the lithium concentration and different lithium compounds formed in the carbon electrode.

As expected, ROHG carbon shows significantly different entropy and enthalpy behavior compared to graphite. From Figure 6, a change in slope for enthalpy is seen around $Li_{0.05}C_6$ for both graphite and ROHG. This observation is concurrent with the OCV curve as shown in Figure 5. This observation suggests that there is change in the order of mechanism of insertion and thereby the products formed. Graphite shows initial entropy of 84.27 $J{\cdot}mol^{-1}{\cdot}K^{-1}$ at −0.800 V. As mentioned earlier, there is a large potential

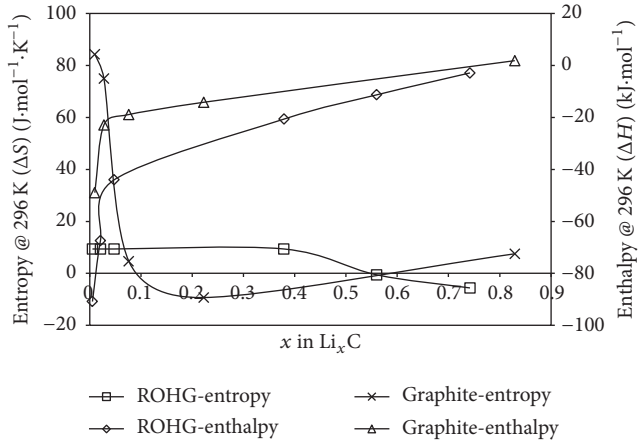

Figure 6: Entropy and enthalpy change with moles of lithium intercalated in anodes.

drop initially from −2.95 V (starting OCV) to −0.800 V. With further lithium intercalation (up to $Li_{0.076}C_6$), the entropy becomes significantly negative (4.68 $J{\cdot}mol^{-1}{\cdot}K^{-1}$) which indicates that there is significant order introduced in the system. With further lithium intercalation, there is more negative shift in the entropy (−9.36 $J{\cdot}mol^{-1}{\cdot}K^{-1}$ with graphite intercalation compound stoichiometry of $Li_{0.222}C_6$) which indicates more ordering of intercalated lithium in graphite. With further intercalation $Li_{0.83}C_6$ forms and the entropy becomes positive (+7.49 $J{\cdot}mol^{-1}{\cdot}K^{-1}$). This indicates some disorder in the system. Overall, the general trend is in agreement with the graphite model seen in the literature [8, 10, 11]. In short, significant change in the entropy is seen in graphite in the initial lithium intercalation process up to ~$Li_{0.1}C_6$ after which the entropy does not change significantly which agrees with literature [13]. However, with ROHG the initial entropy of +9.36 $J{\cdot}mol^{-1}{\cdot}K^{-1}$ at −1.0 V is seen with lithium stoichiometry of $Li_{0.005}C_6$. No change in the entropy occurs with further lithium intercalation and the entropy stays at 9.36 $J{\cdot}mol^{-1}{\cdot}K^{-1}$ until $Li_{0.38}C_6$. This observation suggests that there is a certain relative disorder to the system compared to graphite and the structure always remains random. Further lithium intercalation in ROHG ($Li_{0.75}C_6$) shows some relative ordering of the Li-C compound formed which shifts the entropy to negative values. However, this change is not a significant change in entropy. There is a certain randomness associated with the insertion of lithium in the ROHG structure unlike graphite.

As mentioned earlier, the enthalpy versus lithium concentration data for graphite and ROHG in Figure 6 suggests that though the trends in the change in the enthalpy look similar, there is a more gradual change in the slope of enthalpy curve for ROHG compared to graphite. Lower free energy associated with lithium intercalation suggests easier intercalation and deintercalation in the ROHG carbon structure compared to graphite. The enthalpy change for graphite is from −48.98 kJ mol^{-1} to +1.84 kJ mol^{-1} whereas the enthalpy change for ROHG is from −90.85 kJ mol^{-1} to −2.88 kJ mol^{-1}. Over the entire range of lithium intercalation,

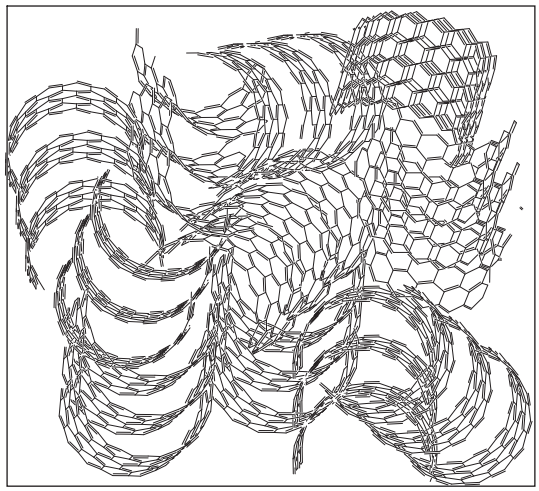

Figure 7: Structure and morphology of ROHG based on Monte Carlo simulations.

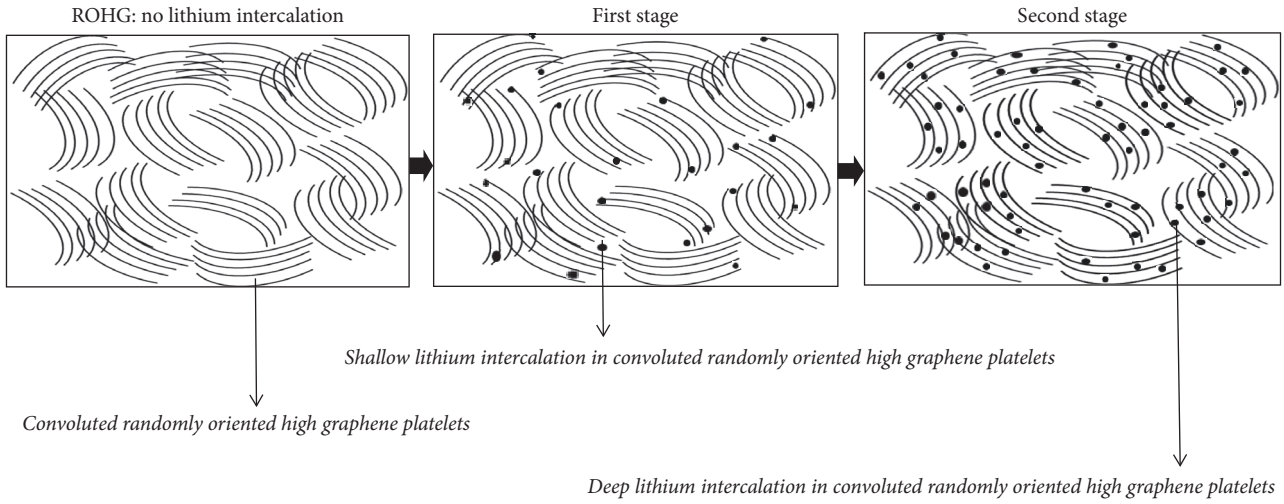

Figure 8: Predicted model for different stages of lithium intercalation in ROHG.

the ROHG shows lower energy associated with lithium intercalation compared to lithium intercalation in graphite. The difference in the enthalpy variation with intercalation between the two materials shows that different species are formed during lithium intercalation in each of the two materials. These changes in the plots presumably originate from the continuously changing chemical environment or bonding of lithium to the platelets in the structure of ROHG carbon with each progression of intercalation of lithium. In the following a model is presented to explain the behavior based on the structure of the ROHG carbon.

3.3. Monte Carlo Simulation of ROHG. A Monte Carlo simulation was done in-house to predict the structure of the ROHG carbon. From the simulation, the ROHG carbon consists of cluster of convoluted and randomly oriented graphene platelets at high concentration as shown in Figure 7 and therefore the carbon is called "Randomly Oriented High Graphene" (ROHG) carbon.

3.4. Lithium Intercalation Model in ROHG. Based on the observations made from the intercalation curves (Figure 4), OCV curves versus lithium mole fraction (Figure 5), entropy (Figure 6), enthalpy (Figure 6), and Monte Carlo model (Figure 7), a model is proposed for lithium intercalation in the structure of ROHG as shown in Figure 8. The lithium insertion takes place in between the cluster of convoluted and randomly oriented graphene platelets. The distance between the graphene platelets in ROHG is larger compared to graphene platelets in graphite which support fast lithium intercalation and deintercalation in the structure of the carbon. During the first stage, lithium is beginning to get intercalated in the platelet structure of ROHG as shown in Figure 8. Further intercalation allows the insertion of lithium deeper in the convoluted platelets.

4. Conclusion

Half cells equilibrated OCV-temperature relationship was explored to investigate the entropy and enthalpy of lithium

intercalation in ROHG carbon and compared to standard graphite material. The change in entropy of lithium intercalation for ROHG carbon was not as significant and minimally dependent on the concentration of lithium in the ROHG structure compared to the standard graphite. Graphite showed dependency on lithium concentration with initial insertion of lithium followed by stabilization in entropy. From enthalpy data, it appears that the energy associated with intercalation of lithium in ROHG is much lower than graphite. Therefore, the intercalation of lithium in ROHG is easier than in graphite. This is advantageous in high rate applications. From the entropy and enthalpy observations, it is concluded that the ROHG carbon has different chemical environment around intercalated lithium compared to graphite. This change is due to the randomly oriented graphene platelets cluster structure of the ROHG carbon compared to the parallel long graphene platelets structure in graphite.

Abbreviations

ROHG: Randomly Oriented High Graphene
OCV: Open Circuit Voltage
GIC: Graphite intercalation compounds
SEI: Solid electrolyte interface
emf: Electromotive force.

Conflicts of Interest

The authors declare that they have no conflicts of interest.

Acknowledgments

This work was supported by Corning Incorporated.

References

[1] J. B. Goodenough and K.-S. Park, "The Li-ion rechargeable battery: a perspective," *Journal of the American Chemical Society*, vol. 135, no. 4, pp. 1167–1176, 2013.

[2] N. Nitta, F. Wu, J. T. Lee, and G. Yushin, "Li-ion battery materials: present and future," *Materials Today*, vol. 18, no. 5, pp. 252–264, 2015.

[3] C. Liu, Z. G. Neale, and G. Cao, "Understanding electrochemical potentials of cathode materials in rechargeable batteries," *Materials Today*, vol. 19, no. 2, pp. 109–123, 2016.

[4] K. Xu, "Electrolytes and interphases in Li-ion batteries and beyond," *Chemical Reviews*, vol. 114, no. 23, pp. 11503–11618, 2014.

[5] T. Ohzuku, Y. Iwakoshi, and K. Sawai, "Formation of lithium-graphite intercalation compounds in nonaqueous electrolytes and their application as a negative electrode for a lithium ion (shuttlecock) cell," *Journal of the Electrochemical Society*, vol. 140, no. 9, pp. 2490–2497, 1993.

[6] J. R. Dahn, R. Fong, and M. J. Spoon, "Suppression of staging in lithium-intercalated carbon by disorder in the host," *Physical Review B*, vol. 42, no. 10, pp. 6424–6432, 1990.

[7] D. Billaud, F. X. Henry, and P. Willmann, "Electrochemical synthesis of binary graphite-lithium intercalation compounds," *Materials Research Bulletin*, vol. 28, pp. 477–483, 1993.

[8] C. Sole, N. E. Drewett, and L. J. Hardwick, "In situ Raman study of lithium-ion intercalation into microcrystalline graphite," *Faraday Discussions*, vol. 172, pp. 223–237, 2014.

[9] S. Konar, U. Häusserman, and G. Svensson, "Intercalation Compounds from LiH and Graphite: Relative Stability of Metastable Stages and Thermodynamic Stability of Dilute Stage I_d," *Chemistry of Materials*, vol. 27, pp. 2566–2575, 2015.

[10] G. R. Williams, A. M. Fogg, J. Sloan, C. Taviot-Guého, and D. O'Hare, "Staging during anion-exchange intercalation into $[LiAl_2(OH)_6]Cl{\cdot}yH_2O$: structural and mechanistic insights," *Dalton Transactions*, no. 32, pp. 3499–3506, 2007.

[11] A. Lerf, "Storylines in intercalation chemistry," *Dalton Transactions*, vol. 43, no. 27, pp. 10276–10291, 2014.

[12] C. J. Wen and R. A. Huggins, "Thermodynamic Study of the Lithium-Tin System," *Journal of the Electrochemical Society*, vol. 128, no. 6, pp. 1181–1187, 1981.

[13] Y. F. Reynier, R. Yazami, and B. Fultz, "Thermodynamics of lithium intercalation into graphites and disordered carbons," *Journal of the Electrochemical Society*, vol. 151, no. 3, pp. A422–A426, 2004.

[14] J. R. Dahn and R. R. Hearing, "Entropy measurements on Li_xTiS_2," *Canadian Journal of Physics*, vol. 61, pp. 1093–1098, 1983.